Eur. Phys. J. B **65**, 1–4 (2008)
DOI: 10.1140/epjb/e2008-00329-0

THE EUROPEAN PHYSICAL JOURNAL B

Infrared reflectivity spectra of η-$Na_{1.3}V_2O_5$ in the charge disordered and ordered phase

Z.V. Popović[1,a], D.M. Đokić[1], Z. Dohčević–Mitrović[1], M. Isobe[2], and Y. Ueda[2]

[1] Center for Solid State Physics and New Materials, Institute of Physics, Pregrevica 118, 11080 Belgrade, Serbia
[2] Materials Design and Characterization Laboratory, Institute for Solid State Physics, The University of Tokyo, 5-1-5 Kashiwanoha, Kashiwa, Chiba 277-8581, Japan

Received 18 December 2007 / Received in final form 13 May 2008
Published online 22 August 2008 –

Abstract. We have measured the far-infrared reflectivity spectra of the sodium vanadium oxide η-$Na_{1.3}V_2O_5$ polycrystals in the wide temperature (80–300 K) and frequency (150–1500 cm^{-1}) range. Appearance of new phonon oscillators, phonon oscillator mode splitting and step-like shift of TO and LO frequencies at low temperatures are correlated with the charge-ordering phase transition, which takes place at about 120 K in this vanadium oxide.

PACS. 78.30.Hv Other nonmetallic inorganics – 63.20.D- Phonon states and bands, normal modes, and phonon dispersion – 71.30.+h Metal-insulator transitions and other electronic transitions – 71.27.+a Strongly correlated electron systems; heavy fermions

1 Introduction

In the sodium-vanadium oxide system $Na_xV_2O_5$, there exist seven phases denoted by α-, β-, δ-, τ-, α'-, η-, and κ-phases in the ascending order of x. They are mixed-valence compounds of V^{4+} (d^1, S = 1/2) and V^{5+} (d^0, S = 0) ions, among which α'-$Na_xV_2O_5$ ($x = 1.0$) has been studied most intensively for its anomalous phase transition like a spin – Peierls transition [1,2]. Recently, it has been reported [3] that the η-phase $Na_xV_2O_5$ ($x \sim 1.3$) exhibits low-dimensional behavior of the magnetic susceptibility. Two models have been proposed to explain the spin gap in this oxide. First one is based on fused chain model [4] of ten-node rings with the spin gap, taking into account the $V_{10}O_{30}$ chains as a basic unit in η-phase. Second model is based on low-temperature structural measurements [5], which have revealed the existence of a structural second-order phase transition in this oxide, associated with a concomitant charge ordering. A doubling of the b lattice parameter observed below 100 K signifies that each magnetic unit contains, at low temperature, 2×9 S = 1/2 spins. Hence the origin of the spin gap can be related to the formation of this superstructure below 100 K in the system.

Many of the physical properties of η-$Na_{1.3}V_2O_5$, including lattice dynamics, are unknown. The X-band electron-spin resonance [6] and complementary magnetic susceptibility data [5] give additional evidence for the transition around 100 K and confirm the existence of the spin gap, which is estimated to be of the order of 35 K. NMR study of spin gap in the vanadium bronze η-$Na_{1.286}V_2O_5$ [7] revealed that spin gap energy is vanadium site dependent. They estimated the gap value of 152 K, 54 K and 174 K for vanadium V(4)A, V(4)B and V(7)A sites, respectively.

In the Raman scattering measurements [8] on single crystal vanadium bronze samples the 27 first-order Raman active modes were observed, as well as their overtones and combinational lines. The appearance of new phonon or spin-related modes is not registered in the low temperature phase. This is explained as a consequence of their small intensity, sample heating by laser irradiation or due to small normal vibrational coordinate change by crystal structure transformation. The temperature dependence of Raman active phonon mode frequency and damping shows step-like shift at low temperatures in the charge ordered phase.

In this paper we measured the infrared reflectivity spectra of polycristalline η-$Na_{1.3}V_2O_5$ in the charge disordered and ordered phase. We found new phonon oscillators, oscillator splitting and step-like frequency shift of infrared active modes by lowering the temperature below the charge ordering temperature (T_{CO}), i.e. the phase transition has a rather strong influence on the phonon dynamics of η-$Na_{1.3}V_2O_5$.

2 Experiment

The present work was performed on powder samples. The details of the sample preparation were published elsewhere [3]. The infrared measurements were carried out

[a] e-mail: zoran.popovic@phy.bg.ac.yu

with a BOMEM DA-8 FTIR spectrometer. A DTGS pyroelectric detector was used to cover the wave number region from 100 to 700 cm^{-1}; a liquid nitrogen cooled HgCdTe detector was used from 500 to 5000 cm^{-1}. Spectra were collected with 2 cm^{-1} resolution, with 1000 interferometer scans added for each spectrum. For low-temperature measurements a Janis STDA 100 cryostat was used.

3 Results and discussion

The η-phase, which can also be denoted by the stoichiometric formula $Na_9V_{14}O_{35}$, crystallizes at room temperature in the monoclinic system (space group $P2/c$) with an original structure built up of layers consisting of VO_5 square pyramids sharing edges and corners, with their apical oxygens pointing up and down alternately to form double zigzag chains in the [100] direction, Figure 1. These double chains are bridged by VO_4 tetrahedra to form the V_2O_5 layers. A peculiarity of the $Na_9V_{14}O_{35}$ crystal structure is shearing of VO_5 chains at every five $V(5)O_5$–$V(5)O_5$ units, as it is illustrated in Figure 1. The Na atoms are located between the layers. The V_2O_5 layers contain V^{4+}, $V^{4.5+}$, and V^{5+} ions. Each $V(i)O_4$ ($i = 4, 7$) tetrahedron has a V^{5+} ion (d^0), each $V(i)O_5$ ($i = 1, 2, 3, 6$) square pyramid has a V^{4+} (d^1) ion, and each $V(5)O_5$ square pyramid has a $V^{4.5+}$ ion. The low-temperature structure remains centrosymmetric with space group $P2/c$ but with a doubled b lattice parameter, as we have already mentioned. Two vanadium sites which host $V^{4.5+}$ ions at room temperature become stabilized as one V^{4+} and one V^{5+} at low temperature.

The P-centered monoclinic unit cell [3] of $Na_9V_{14}O_{35}$ consists of two formula units ($Z = 2$) comprising 116 atoms in all. Since there is a large number of atoms in the unit cell and low symmetry of $P2/c$ (C_{2h}^4) space group we can expect a large number of optically active modes. The factor-group-analysis [8] yields the total number of optical active phonons in $Na_9V_{14}O_{35}$:

$$\Gamma^{opt.}_{Na_9V_{14}O_{35}} = 86A_g(xx, yy, zz, xz) + 88B_g(xy, yz) + 85A_u(\mathbf{E}||\mathbf{y}) + 86B_u(\mathbf{E} \perp \mathbf{y}).$$

According to this representation one can expect totally 171 infrared active modes to be observed in the infrared experiment.

Figure 2 shows the unpolarized reflectivity spectra of η-$Na_{1.3}V_2O_5$ polycrystalline samples measured at room and liquid nitrogen temperatures in the spectral range from 150 to 1150 cm^{-1}. These spectra contain both the A_u and B_u symmetry modes. We have observed 30 oscillators at room temperature and additional 6 more oscillators at 80 K (in the charge ordered state). The frequencies of TO and LO modes are given in Table 1. These frequencies were obtained by Kramers-Kronig Analysis (KKA) and first derivative (FD) of the reflectivity spectra. Because of many very weak oscillators in relatively narrow spectral range or weak intensity oscillators close to high intensity one the KKA turned to be insensitive to detect TO and LO frequencies of all observed oscillators. Therefore, we

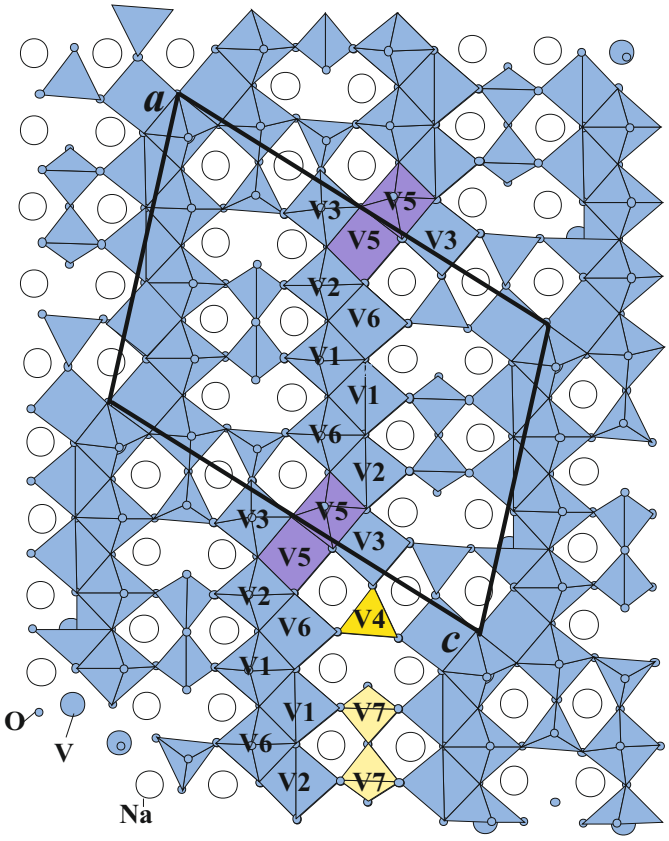

Fig. 1. Crystal structure of η-$Na_{1.3}V_2O_5$ projected on the (ac) plane. The VO_5-chains running parallel to the a-axis.

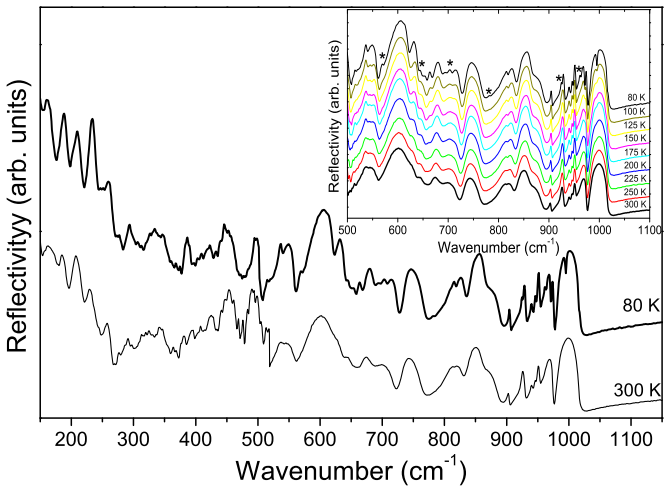

Fig. 2. Unpolarized far-infrared reflectivity spectra of η-$Na_{1.3}V_2O_5$ measured at room and liquid nitrogen temperature. Inset: Infrared reflectivity spectra at different temperatures.

calculated FD of the reflectance data as a complementary method. The advantage of using the derivative technique is well documented in references [9,10]. In Figure 3, for the highest frequency oscillators, we have compared the derivative spectrum with the optical conductivity and loss function data obtained from KKA. It is obvious that maxima (minima) of the DT spectrum correspond to maxima

Table 1. Phonon mode frequencies (in cm^{-1}) of η-$Na_{1.3}V_2O_5$.

Raman [8]		Infrared		Tentative assignment
A_g	B_g	TO	LO	
162		159.4	174.0	
213		180.0	191.1	
232		199.7	216.8	
250		227.1	238.3	
309		252.8	263.1	
321		274.3	277.7	O–V–O bending
333		288.8	293.1	
355		340.0	348.0	
377		374.6	383.1	
400		419.1	429.4	
439		438.0	462.8	
466				
484		486.0	501.4	
514		511.7	518.6	
527		531.3	554.4	
565		585.3	615.2	
648		625.8	634.7	$V–O_5$ stretching in the basal plane
		640.3	648.0	
		668.2	680.0	
		694.3	716.4	
		730.9	759.8	
		803.2	813.8	
811	817	817.7	826.4	
823				
849		867.8	884.2	
900		900.6	904.5	$V–O_4$ stretching
931		923.8	928.6	
		938.2	941.1	
943		944.0	946.9	
948		949.0	952.7	
964		961.4	973.9	$V–O_5$ stretching
990		979.7	1016.3	

of the optical conductivity – TO modes (loss function – LO modes). Since reflectivity measurements carried out on powder samples give good results for TO and LO mode frequencies in the case of isolated oscillators only, the obtained frequencies from Table 1 should be taken as tentative ones, only. Namely, two or more oscillators from different symmetries can appear as multi-peak-structure in the reflectivity spectra of powder samples [11]. Because of that, the assignment of the infrared-active modes is practically impossible without polarized measurements on single crystals.

If we compare this reflectivity spectra with the infrared reflectivity spectra of other vanadates [11,12], we can conclude that the two highest frequency modes, as well as the modes between 500 and 700 cm^{-1}, represent the vibration of VO_5 pyramid. The modes between 750 and 950 cm^{-1} are bond stretching vibrations of VO_4 tetrahedra. In the

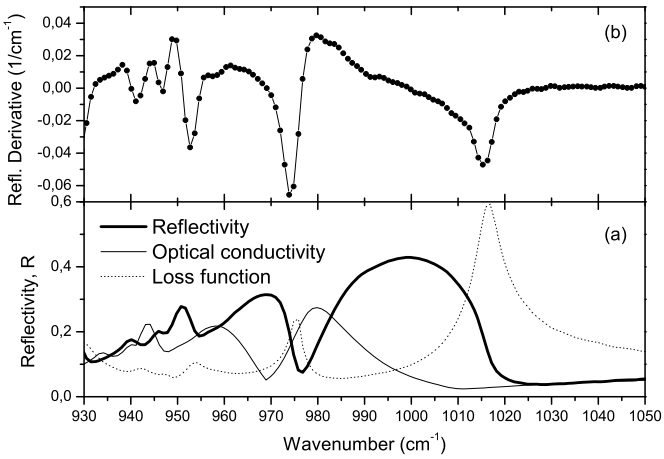

Fig. 3. (a) Unpolarized infrared reflectivity spectra of η-$Na_{1.3}V_2O_5$ in the 930–1050 cm^{-1} spectral range together with optical conductivity and loss function ($-Im[1/\epsilon(\omega)]$), obtained using KKA of the reflectivity data. (b) First derivative of the reflectivity spectrum of η-$Na_{1.3}V_2O_5$.

spectral range below 500 cm^{-1} there are many modes that originate from V–O bond bending vibration. As in the case of Raman spectra [8] the more precise assignment of infrared active modes is not possible without single crystal measurements.

By lowering the temperature the observed modes harden and strong phonon oscillators start decomposing into several modes. At temperatures below 125 K new modes appear (denoted by asterisk in the inset of Fig. 2), as a consequence of phase transition. This finding is in accordance with the X-ray measurements of η-$Na_{1.3}V_2O_5$ in the charge ordered state [5]. Namely, due to the doubling of the b-axis below phase transition temperature it is natural to expect an appearance of new phonon oscillators.

Figure 4 (left panel) presents the infrared reflectivity spectra of $Na_9V_{14}O_{35}$ in the spectral range between 955 and 1030 cm^{-1} at different temperatures. The decomposition of the 970 and 1000 cm^{-1} oscillators into several other ones starts at temperatures lower than 200 K, see Figure 4, right panel. Because these new oscillators appear at temperatures much higher than the critical temperature T_{CO} we concluded that they were masked by stronger oscillators at room temperature and became observable due to reduction of broadening of stronger oscillators with temperature decrease. At temperatures close to the phase transition temperature the only one additional mode appears in this spectral range, which is denoted by asterisk in Figure 4.

In order to examine the influence of the phase transition to the phonon properties of $Na_9V_{14}O_{35}$ we analyzed LO mode frequency vs temperature change of an isolated oscillator, Figure 5. With temperature lowering LO mode frequency increases monotonously from room temperature to the phase transition temperature, when a change of frequency is observed. The drastic frequency variation is a consequence of the charge ordering, i.e. the change of crystal and magnetic structure at the phase

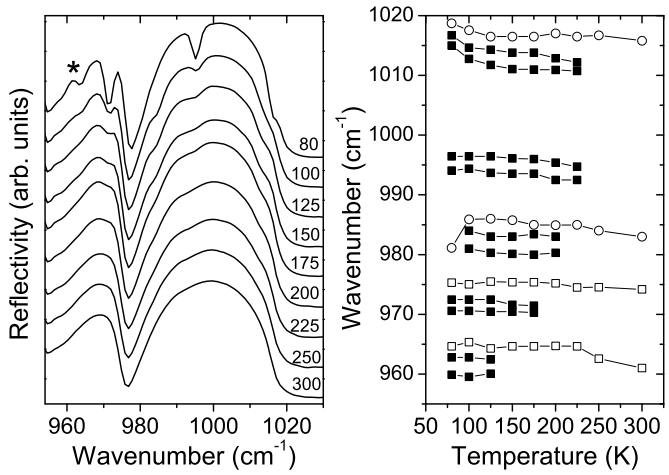

Fig. 4. Left panel: unpolarized infrared reflectivity spectra of η-$Na_{1.3}V_2O_5$ in the 955–1030 cm^{-1} spectral range. Right panel: temperature dependence of TO and LO mode frequency of several oscillators in the 955–1030 cm^{-1} spectral range.

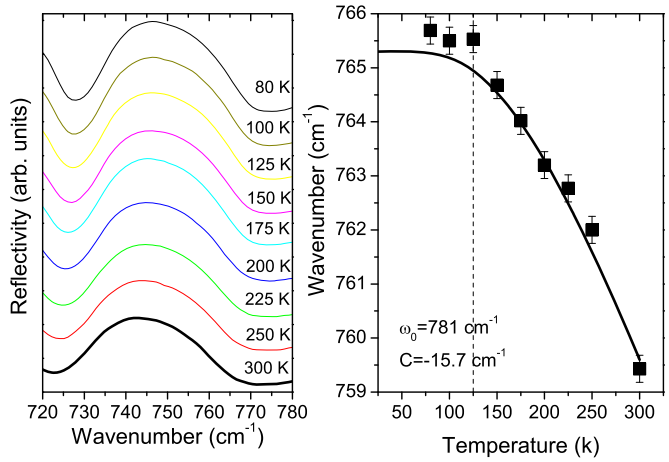

Fig. 5. Left panel: unpolarized infrared reflectivity spectra of η-$Na_{1.3}V_2O_5$ in the 720–780 cm^{-1} spectral range. Right panel: temperature dependence of LO mode frequency of the phonon oscillator from the left panel. Solid line represents the anharmonic phonon-phonon interaction spectrum, equation (1).

transition due to the spin gap opening. In order to distinguish the phonon-phonon contribution due to the anharmonic effects from charge ordering-related contribution we have fitted the high temperature part of the frequency versus temperature dependence using a model for the anharmonic phonon-phonon interaction [13]:

$$\omega_{ph}(T) = \omega_0 + C[1 + 2/(e^{\omega_0/2kT} - 1)], \qquad (1)$$

where ω_0 and C take the values 781 cm^{-1} and –15.7 cm^{-1}, for the LO mode under consideration. The calculated spectra are represented by solid line in Figure 5 (right panel). It is obvious that the dominant contribution in the frequency versus temperature dependence of this LO mode below the phase transition arises from charge ordering and not only from phonon-phonon interaction due to the anharmonic effects.

In conclusion, we have measured unpolarized far-infrared reflectivity spectra of η-$Na_{1.3}V_2O_5$ polycrystals in the wide temperature and frequency range. The appearance of new infrared active phonon modes, mode splitting and the phonon frequency variation, below 120 K, are interpreted as a consequence of the change of crystal structure at the phase transition due to the charge ordering.

This work was supported by the Serbian Ministry of Science under Project No. 141047, the CoMePhS-517039 STREP Project and COST P16 Programme. We would like to express our thanks to A. Milutinović for the help with KKA.

References

1. M. Isobe, Y. Ueda, J. Phys. Soc. Jpn. **65**, 1178 (1996)
2. M. Isobe, Y. Ueda, K. Takizawa, T. Goto, J. Phys. Soc. Jpn. **67**, 755 (1998)
3. M. Isobe, Y. Ueda, Y. Oka, T. Yao., J. Solid State Chem. **145**, 361 (1999)
4. M.-H. Whangbo, H.-J. Koo, Solid State Commun. **115**, 115 (2000)
5. F. Duc, P. Millet, S. Ravy, A. Thiollet, F. Chabre, A.M. Ghorayeb, F. Mila, A. Stepanov, Phys. Rev. B **69**, 094102 (2004)
6. F. Chabre, A.M. Ghorayeb, P. Millet, V.A. Pashchenko, A. Stepanov, Phys. Rev. B **72**, 012415 (2005)
7. T. Hayashi, T. Nakamura, T. Kozuka, M. Itoh, M. Isobe, J.I. Yamura, Y. Ueda, J. Mag. Mag. Materials **310**, 1224 (2007)
8. Z.V. Popović, V.V. Moshchalkov, M. Isobe, Y. Ueda, Solid State Commun. **142**, 385 (2007)
9. D.J. Lockwood, G. Yu, N.L. Rowell, Solid State Commun. **136**, 404 (2005)
10. G. Yu, N.L. Rowell, D.J. Lockwood, Z.R. Wasilewski, Appl. Phys. Lett. **83**, 3683 (2003)
11. Z.V. Popović, M.J. Konstantinović, R. Gajić, V.N. Popov, M. Isobe, Y. Ueda, V.V. Moshchalkov, Phys. Rev. B **65**, 184303 (2002)
12. Z.V. Popović, V. Stergiou, Y.S. Raptis, M.J. Konstantinović, M. Isobe, Y. Ueda, V.V. Moshchalkov, J. Phys.: Cond. Matter **14**, L583 (2002)
13. M. Balkanski, R.F. Wallis, E. Haro, Phys. Rev. B **28**, 1928 (1983)